

Approximating Full Conformal Prediction at Scale via Influence Functions

Javier Abad^{1,2}, Umang Bhatt^{1,3}, Adrian Weller^{1,3}, Giovanni Cherubin⁴

¹ University of Cambridge, UK

² ETH Zurich, Switzerland

³ The Alan Turing Institute, London, UK

⁴ Microsoft Research, Cambridge, UK

javier.abadmartinez@ai.ethz.ch, {usb20, aw665}@cam.ac.uk, giovanni.cherubin@microsoft.com

Abstract

Conformal prediction (CP) is a wrapper around traditional machine learning models, giving coverage guarantees under the sole assumption of exchangeability; in classification problems, for a chosen significance level ε , CP guarantees that the error rate is at most ε , irrespective of whether the underlying model is misspecified. However, the prohibitive computational costs of “full” CP led researchers to design scalable alternatives, which alas do not attain the same guarantees or statistical power of full CP. In this paper, we use influence functions to efficiently approximate full CP. We prove that our method is a consistent approximation of full CP, and empirically show that the approximation error becomes smaller as the training set increases; e.g., for 10^3 training points the two methods output p-values that are $< 10^{-3}$ apart: a negligible error for any practical application. Our methods enable scaling full CP to large real-world datasets. We compare our full CP approximation (ACP) to mainstream CP alternatives, and observe that our method is computationally competitive whilst enjoying the statistical predictive power of full CP.

1 Introduction

Conformal prediction (CP) is a post-hoc approach to providing validity guarantees on the outcomes of machine learning (ML) models; in classification, an ML model wrapped with “full” CP outputs prediction sets that contain the true label with (chosen) probability $1 - \varepsilon$, under mild distribution assumptions. Unfortunately, full CP is notoriously computationally expensive. Many have proposed alternative methods to avoid the full CP objective; these include: split (or “inductive”) CP (Papadopoulos et al. 2002), cross-CP (Vovk 2012), jackknife+ (Barber et al. 2021), RAPS (Angelopoulos et al. 2020), CV+ (Romano, Sesia, and Candes 2020). While these methods have shown practical promise, they do not attain the same validity guarantee as full CP or its statistical power (e.g., prediction set size). Recent work optimized full CP for ML models that support incremental and decremental learning by speeding up the leave-one-out (LOO) procedure required for the prediction set calculation (Cherubin, Chatzikokolakis, and Jaggi 2021); however, this approach may not scale to complex models such as neural networks.

Herein, we first discuss how to approximate the full CP objective. We focus on full CP for classification, and optimize it for ML models trained via ERM (e.g., logistic regression, neural networks). The key insight we leverage is that, for each test point, full CP: (i) retrains the underlying ML model on the additional test point, and (ii) performs a LOO procedure for each training point. We observe we can approximate both steps, and avoid retraining each time, by using first order influence functions (Hampel 1974). We term our method *Approximate full Conformal Prediction* (ACP), and we prove finite-sample error guarantees: as the training set grows, ACP approaches full CP. We then show that a stronger regularization parameter for training the underlying ML model improves the approximation quality.

We empirically demonstrate that ACP is competitive with existing methods on MNIST (LeCun 1998), CIFAR-10 (Krizhevsky, Nair, and Hinton 2009), and US Census (Ding et al. 2021). Unlike full CP, ACP scales to large datasets for real-world ML models (logistic regression, multilayer perceptrons, and convolutional neural networks). Performance-wise, ACP is consistently better than existing alternatives in terms of statistical power: it attains the desired error rate ε with tighter prediction sets; Figure 1 shows on CIFAR-10 examples where, unlike other methods, ACP learns smaller prediction sets that still contain the true label.

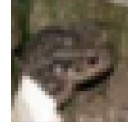
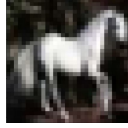
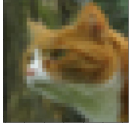
2 Preliminaries

We describe full CP, and then introduce influence functions, our main optimization tool.

2.1 Notation and full CP

Consider a training set $Z = (X, Y) \in (\mathcal{X} \times \mathcal{Y})^N$. For a test object $x \in \mathcal{X}$ and a chosen significance level $\varepsilon \in [0, 1]$, a CP returns a set $\Gamma_x^\varepsilon \subseteq \mathcal{Y}$ containing x ’s true label with probability at least $1 - \varepsilon$. This guarantee (*validity*) holds for any exchangeable distribution on $Z \cup \{(x, y)\}$. Since the error rate of a CP is guaranteed by validity, a data analyst only needs to control the tightness (*efficiency*) of its prediction set; average $|\Gamma_x^\varepsilon|$ is a common efficiency criterion (Vovk et al. 2016). Efficiency is controlled by improving the underlying model that CP wraps.

Underlying model. A CP can be built around virtually any ML model θ . We assume the underlying model is trained via



Method	Prediction set	Method	Prediction set	Method	Prediction set
ACP	bird, <u>cat</u> , deer, frog	ACP	auto, cat, frog, <u>horse</u> , truck	ACP	cat, deer, <u>frog</u> , horse
SCP	bird, deer, frog	SCP	auto, deer, frog, truck	SCP	cat, deer, dog, <u>frog</u> , horse, truck
RAPS	bird, <u>cat</u> , deer, dog, frog	RAPS	plane, auto, bird, deer, frog, ship, truck	RAPS	cat, deer, dog, <u>frog</u> , horse, truck
CV+	bird, <u>cat</u> , deer, dog, frog	CV+	plane, auto, deer, frog, <u>horse</u> , truck	CV+	cat, deer, dog, <u>frog</u> , horse

Figure 1: Prediction sets generated by CP methods ($\varepsilon = 0.2$) for CIFAR-10 examples. Our method (ACP) yields prediction sets that (1) contain the true label and (2) are the smallest. ACP approximates well full CP in large training sets, such as CIFAR-10, inheriting its statistical power.

ERM by minimizing the risk: $R(Z, \hat{\theta}) \equiv \frac{1}{N} \sum_{z_i \in Z} \ell(z_i, \hat{\theta})$; $\ell(z, \theta)$ is the loss of the model at a point z , which we assume to be convex and twice differentiable in θ . This assumption holds for many popular loss functions. Let $\theta_Z \equiv \operatorname{argmin}_{\theta \in \Theta} R(Z, \hat{\theta})$ be the ERM solution; we assume θ_Z to be unique, and discuss relaxations in Section 7.

Nonconformity measure. The underlying model is used to construct a nonconformity measure, which defines a CP. A nonconformity measure is a function $A : (\mathcal{X} \times \mathcal{Y}) \times (\mathcal{X} \times \mathcal{Y})^N \rightarrow \mathbf{R}$ which scores how *conforming* (or *similar*) an example (x, y) is to a bag of examples \bar{Z} . We focus on the two most common ways of defining nonconformity measures (and, hence, CP) on the basis of a model: the *deleted* and the *ordinary* scheme (Vovk, Gammerman, and Shafer 2005).

Full CP (deleted). Consider example \hat{z} and a training set Z . The nonconformity measure can be defined from the deleted (LOO) prediction: $A(z_i, Z) = \ell(z_i, \theta_{Z \cup \{\hat{z}\} \setminus \{z_i\}})$, for all $z_i \in Z \cup \{\hat{z}\}$. Computing this nonconformity measure requires training the model on $Z \cup \{\hat{z}\} \setminus \{z_i\}$. This scheme computes the loss at a point after removing it from the model’s training data.

Algorithm 1 shows how the nonconformity measure is used in full CP. For a test point x , CP runs a statistical test for each possible label $\hat{y} \in \mathcal{Y}$ to decide if it should be included in the prediction set Γ_x^ε . The statistical test requires computing a nonconformity score α_i by running A for each point in the *augmented* training set $Z \cup \{(x, \hat{y})\}$; then, a p-value is computed, and a decision is taken based on the threshold ε . This algorithm is particularly expensive. Crucially, for each test point, and for every candidate label, one needs to retrain the underlying ML model $N + 1$ times.

Full CP (ordinary). A computationally faster scheme is achieved by taking the loss at the point: $A(z_i, Z) = \ell(z_i, \theta_{Z \cup \{\hat{z}\}})$. We refer to this as the *ordinary* scheme (Algorithm 3). This method is inherently faster than the deleted approach, as it only requires training one model per test example and candidate label. However, the ordinary scheme generally leads to less efficient predictions (Section 5).

Optimizing CP. The complexity of full CP depends on: (i) the number of training points N , and (ii) the number of labels $|\mathcal{Y}|$. Optimizing w.r.t. $|\mathcal{Y}|$ is necessary for regression settings, where full CP is not applicable directly; this was done, for

specific choices of nonconformity measures, by Papadopoulos, Vovk, and Gammerman (2011); Nouretdinov, Melluish, and Vovk (2001); Lei (2019); Ndiaye and Takeuchi (2019); Ndiaye (2022). Our work focuses on optimizing w.r.t. N ; this enables applying full CP classification to large datasets. Future work may combine our optimizations and CP regression strategies to obtain faster regressors on large training sets (e.g., Cherubin, Chatzikokolakis, and Jaggi 2021).

2.2 Influence functions

Influence functions (IF) are at the core of our proposal. For a training example $z_i \in Z$, let $I_\theta(z_i) = -\frac{1}{N} H_\theta^{-1} \nabla_\theta \ell(z_i, \theta)$ be the *influence* of z_i on model θ , where $H_\theta = \nabla_\theta^2 R(Z, \theta)$ is the Hessian; by assumption, H_θ exists and is invertible. A standard result by Hampel (1974) shows that:

$$\theta_{Z \setminus \{z_i\}} - \theta \approx -I_\theta(z_i). \quad (1)$$

I_θ says how much z_i affects θ during training. We can apply influence functions for computing the influence of a point z_i on any functional. In our work, we are interested in the influence on the loss function at a point z . Let $I_\ell(z, z_i) = \nabla_\theta \ell(z, \theta)^\top I_\theta(z_i)$. Then, similarly to above, we have

$$\ell(z, \theta_{Z \setminus \{z_i\}}) - \ell(z, \theta) \approx -I_\ell(z, z_i). \quad (2)$$

3 Approximate full Conformal Prediction

Our proposal (ACP) hinges on approximating the nonconformity scores via IF. We describe our approach, and prove theoretical results on its consistency and approximation error.

3.1 Approach

The bottleneck of running full CP is the computation of the nonconformity scores $\alpha_i = \ell(z_i, \theta_{Z \cup \{\hat{z}\} \setminus \{z_i\}})$. Each score is determined by computing the loss of the model at point $z_i \in Z \cup \{\hat{z}\}$ after adding point \hat{z} and removing point z_i from the model’s training data Z . There are two ways to approximate α_i via IF: we can approximate the contribution of adding and removing the points to the learned model θ_Z , and then evaluate its loss at z_i (*indirect* approach), or we can directly approximate the contribution of the points on the loss function (*direct* approach). We describe both below.

Algorithm 1: Full CP

```

1: for  $x$  in test points do
2:   for  $\hat{y} \in \mathcal{Y}$  do
3:      $\hat{z} = (x, \hat{y})$ 
4:     for  $z_i \in Z \cup \{\hat{z}\}$  do
5:        $\theta_{Z \cup \{\hat{z}\} \setminus \{z_i\}} = \operatorname{argmin}_{\theta \in \Theta} R(Z \cup \{\hat{z}\} \setminus \{z_i\}, \theta)$ 
6:        $\alpha_i = \ell(z_i, \theta_{Z \cup \{\hat{z}\} \setminus \{z_i\}})$ 
7:     end for
8:      $p(x, \hat{y}) = \frac{\#\{i=1, \dots, N+1 : \alpha_i \geq \alpha_{N+1}\}}{N+1}$ 
9:     If  $p(x, \hat{y}) > \varepsilon$ , include  $\hat{y}$  in set  $\Gamma_x^\varepsilon$ 
10:   end for
11: end for

```

Algorithm 2: Approximate full CP (ACP)

```

1:  $\theta_Z = \operatorname{argmin}_{\theta \in \Theta} R(Z, \theta)$ 
2: for  $x$  in test points do
3:   for  $\hat{y} \in \mathcal{Y}$  do
4:      $\hat{z} = (x, \hat{y})$ 
5:     for  $z_i \in Z \cup \{\hat{z}\}$  do
6:        $\tilde{\alpha}_i = \text{Approximate via Eq. 3 or 4}$ 
7:     end for
8:      $p(x, \hat{y}) = \frac{\#\{i=1, \dots, N+1 : \tilde{\alpha}_i \geq \tilde{\alpha}_{N+1}\}}{N+1}$ 
9:     If  $p(x, \hat{y}) > \varepsilon$ , include  $\hat{y}$  in set  $\Gamma_x^\varepsilon$ 
10:   end for
11: end for

```

Figure 2: Full CP (left) and our proposal, ACP, (right). In ACP, the underlying ML model is only trained once, and nonconformity scores are approximated via influence functions in Line 6.

Indirect approach. We can use Equation 1 to approximate model $\theta_{Z \cup \{\hat{z}\} \setminus \{z_i\}}$ and then compute its loss. That is, let $\tilde{\theta}_{Z \cup \{\hat{z}\} \setminus \{z_i\}} \equiv \theta_Z + I_{\theta_Z}(\hat{z}) - I_{\theta_Z}(z_i)$. Then:

$$\alpha_i \approx \ell(z_i, \tilde{\theta}_{Z \cup \{\hat{z}\} \setminus \{z_i\}}). \quad (3)$$

Direct approach. We can directly compute the influence on the loss. Let θ_Z be a model trained via ERM on the entire training set Z . The direct approximation for the score is:

$$\alpha_i \approx \tilde{\ell}(z_i, \theta_{Z \cup \{\hat{z}\} \setminus \{z_i\}}) \equiv \ell(z_i, \theta_Z) + I_\ell(z_i, \hat{z}) - I_\ell(z_i, z_i). \quad (4)$$

$I_\ell(z_i, \hat{z})$ and $-I_\ell(z_i, z_i)$ are the influence of including point \hat{z} and excluding z_i (Equation 2). Algorithm 2 (ACP) shows how both approaches enable approximating full CP.

ACP gives a substantial speed-up over full CP. In contrast to full CP, ACP has a training phase, in which we: compute the Hessian, the gradient for each point z_i , and provisional scores $\ell(z_i, \theta_Z)$ for $z_i \in Z$. For predicting a test point \hat{z} , it suffices to compute its influence by using the Hessian and gradients at z_i and \hat{z} , which is cheap, and update the provisional scores (see time complexities in Table 4). This enables ACP to scale to large real-world datasets such as CIFAR-10 (Section 5). As a reference, running full CP for the synthetic dataset (Section 4) with 50 features, 1000 training points, and 100 test points took approximately 5 days, whereas ACP took less than 1 hour (CPU time with an Intel Core i7-8750H).

3.2 Theoretical analysis

In this section, we establish the consistency of ACP: its approximation error gets smaller as the training set grows. Further, we study its *finite-sample* validity, and how the underlying model’s regularization parameter affects its approximation error. The consistency of ACP for the indirect approach comes from a result by Giordano et al. (2019). Proving consistency for the direct approach requires a condition, which we state in the next part as a conjecture.

Direct approximation is better than indirect We conjecture that the direct approach approximates better than the indirect one. Intuitively, it is much easier to approximate

the loss at a point (direct) than to estimate the effect of a training point on the model weights, which lay in a high-dimensional space (indirect). We observed this conjecture to hold consistently across a number of simulations (Section 4). Formally:

Condition 1. Assume that the loss ℓ is convex and differentiable. Then the direct method (Equation 4) is a better approximation than the indirect one (Equation 3). That is, let $\alpha_i = \ell(z_i, \theta_{Z \cup \{\hat{z}\} \setminus \{z_i\}})$; then:

$$|\tilde{\ell}(z_i, \theta_{Z \cup \{\hat{z}\} \setminus \{z_i\}}) - \alpha_i| \leq |\ell(z_i, \tilde{\theta}_{Z \cup \{\hat{z}\} \setminus \{z_i\}}) - \alpha_i|.$$

Without Condition 1, we can prove consistency for the indirect approach, but not for the direct approach.

Consistency of ACP We show that ACP is a consistent estimator of full CP. We establish this equivalence in the most generic form possible: we demonstrate that nonconformity scores produced by Algorithm 2 approximate those produced by full CP. In turn, the p-values (and, consequently, error rates) of the two methods get increasingly closer.

Our result is an extension of the work by Giordano et al. (2019), who showed that IF consistently estimate a model’s parameters in a LOO setting. This result holds under a set of assumptions (Assumption 1 in Appendix B), which Giordano et al. (2019) showed to hold for a variety of settings; e.g., they hold when Z are well-behaved IID data and $\ell(\cdot, \theta)$ is an appropriately smooth function. Note that Assumption 1 limits the set of applicable nonconformity measures, e.g., by assuming them to be continuously differentiable.

Theorem 2 (Consistency of approximate full CP). *Under Assumption 1 and Condition 1, let $\alpha_i = \ell(z_i, \theta_{Z \cup \{\hat{z}\} \setminus \{z_i\}})$, and suppose ℓ is K -Lipschitz. For every N there is a constant C such that for every $z_i \in Z \cup \{\hat{z}\}$:*

$$|\tilde{\ell}(z_i, \theta_{Z \cup \{\hat{z}\} \setminus \{z_i\}}) - \alpha_i| \leq KC \frac{\max\{C_g, C_h\}^2}{N},$$

for finite constants C_g, C_h s.t. $\sup_{\theta \in \Theta} \frac{1}{\sqrt{N}} \|\nabla_\theta \ell(z, \theta)\|_2 \leq C_g$ and $\sup_{\theta \in \Theta} \frac{1}{\sqrt{N}} \|\nabla_\theta^2 \ell(z, \theta)\|_2 \leq C_h$.

This result gives a finite-sample bound for the error of the direct approach for ACP; the error of the indirect approach is also bounded as a byproduct of the same proof. We conclude that, as N grows, ACP’s scores get increasingly closer to those produced by full CP. We evaluate this in Section 4.

Validity of ACP Lin, Trivedi, and Sun (2021) state that *finite-sample* validity is not guaranteed when the LOO is estimated with IF since they cannot be exactly computed. They exemplify this issue in the Discriminative Jackknife (Alaa and Van Der Schaar 2020), which approximates the IF using Hessian-Vector-Products (Pearlmutter 1994).

Although we alleviate part of the issue by computing the exact Hessian, we cannot guarantee that our LOO estimation is exact. Basu, Pope, and Feizi (2021) also summarize several issues with using IF in deep learning. Nevertheless, ACP still inherits the high efficiency of full CP, and we observe that validity holds in practice (Section 5). Future work can prove if the approximate scores follow the same distribution as the true ones and, consequently, if exchangeability still holds.

Relation to regularization parameter By extending a result by Koh et al. (2019), we investigate the effect of the ERM regularization parameter on ACP’s approximation error. This result makes fairly simplistic assumptions (Appendix B.2).

Theorem 3 (Approximation goodness w.r.t. regularizer). *Suppose the model is trained via ERM with regularization parameter λ . Under the assumptions of Proposition 5, Assumption 2, and neglecting $\mathcal{O}(\lambda^{-3})$ terms, we have the following cone constraint between the true nonconformity measure $\alpha_i = \ell(z_i, \theta_{Z \cup \{\hat{z}\} \setminus \{z_i\}})$ and its direct approximation $\tilde{\ell}(z_i, \theta_{Z \cup \{\hat{z}\} \setminus \{z_i\}}) \equiv \ell(z_i, \theta_Z) + I_\ell(z_i, \hat{z}) - I_\ell(z_i, z_i)$, where $g(\lambda) = (1 + 3\sigma_{max}/2\lambda + \sigma_{max}^2/2\lambda^2)$, and σ_{max} is the maximum eigenvalue of the Hessian H :*

$$\ell(z_i, \theta_Z) + I_\ell(z_i, \hat{z}) - g(\lambda)I_\ell(z_i, z_i) \leq \alpha_i \leq \tilde{\ell}(z_i, \theta_{Z \cup \{\hat{z}\} \setminus \{z_i\}}).$$

4 Experiments on synthetic data

We study the properties of ACP outlined in Section 3.2 on synthetic data (Appendix C); the underlying model is logistic regression with cross-entropy loss. Results are averaged across 100 test points.

Direct and indirect approximation. We empirically evaluate Condition 1, which claims that the direct method (Equation 4) is never worse than indirect (Equation 3). Figure 3 shows the absolute distance between full CP and ACP’s nonconformity scores as a function of the training set size. Results confirm that direct is always better than indirect, although the two get close for large N . Importantly, the nonconformity scores produced by ACP get increasingly better at approximating those of full CP as the training set grows (cf. Theorem 2). We shall now focus on the direct approach.

Approximation goodness. We evaluate how well ACP approximates full CP, under various parameter choices, as the training set grows. Figure 4a shows the difference between the nonconformity scores of full CP and ACP as the number of features ranges in 5-100. The number of features does impact the IF approximation, although the error becomes

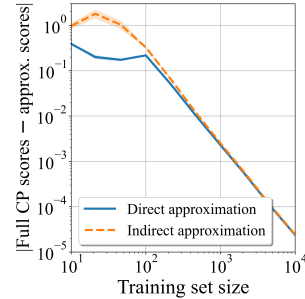


Figure 3: Comparison between direct and indirect approximations. We show the difference between the nonconformity scores of full CP and their approximation as a function of the training set size, averaged across 100 test points. These results support that the direct method is never worse than the indirect (Condition 1), and that both approximate full CP increasingly better (Theorem 2). The standard deviation for the direct approach (blue) is negligible.

negligible as the training set increases. Theorem 3 shows that, unsurprisingly, a larger λ (i.e., stronger regularization) implies better approximation. We confirm this in Figure 4b. Our analysis focuses on the approximation error between nonconformity scores; yet, we remark that a small error between scores implies a more fundamental equivalence between full CP and ACP: their p-values should also have a small distance.

Figure 4c compares full CP and ACP’s p-values. The difference is smaller than 10^{-3} with a training set of 600, and it becomes negligible with $N = 10k$ training examples. Observe that in CP the p-value is thresholded by the significance value ε to obtain a prediction (Algorithm 1). As practitioners are generally interested in values ε with no more than 2 decimals of precision (e.g., $\varepsilon = 0.15$), we argue that an approximation error smaller than 10^{-3} between p-values is more than sufficient for any practical application. Figure 4d compares the error rate (for $\varepsilon = 0.1$) between full CP and ACP. We observe that, after 500 training points, the two methods have the same error.

5 Experiments with real data

We compare mainstream CP alternatives with ACP on the basis of their predictive power (efficiency). Because of its computational complexity, it is infeasible to include full CP in these experiments. Nevertheless, given the size of the training data, the consistency of ACP (Theorem 2), and the results in Section 4, we expect ACP to perform similarly to full CP.

5.1 Existing alternatives to Full CP

There are several alternative approaches to CP for classification. In this work, we compare ACP with:

- Split (or “inductive”) Conformal Prediction (SCP) (Papadopoulos et al. 2002) works by dividing the training set into *proper training set* and *calibration set*. The model is fit on the proper training set, and the calibration set is used to compute the nonconformity scores.
- Regularized Adaptive Prediction Sets (RAPs) (Angelopoulos et al. 2020), is a regularized version of Adap-

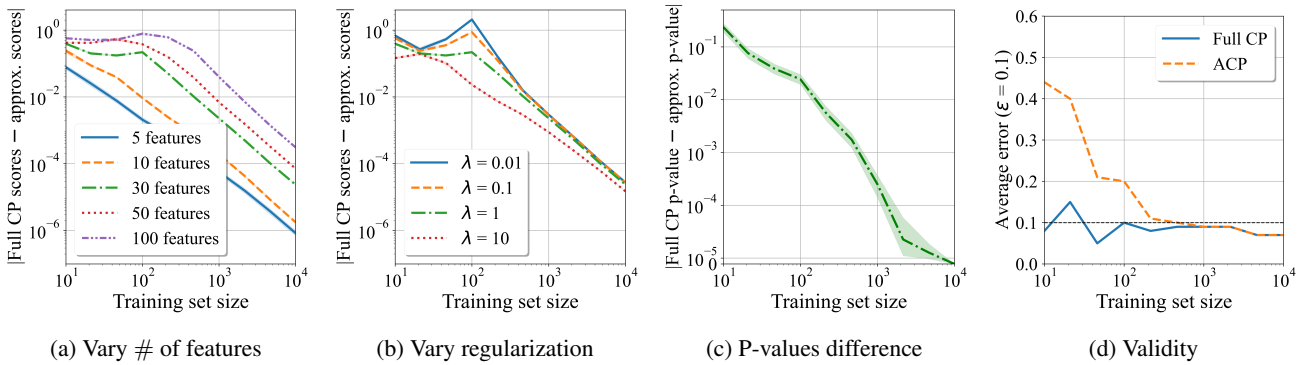


Figure 4: Difference in nonconformity scores for different numbers of features (4a) and for various regularization strengths (4b). The differences in scores are averaged across 100 test points. We also report the difference between p-values (4c) and error rate (4d).

tive Prediction Sets (APS) (Romano, Sesia, and Candes 2020). APS constructs *Generalized inverse quantile conformity scores* from a calibration set adaptively w.r.t. the data distribution. RAPS uses regularization to minimize the prediction set size while satisfying validity.

- Cross-validation+ (CV+) (Romano, Sesia, and Candes 2020) exploits a cross-validation approach while constructing the conformity scores similarly to APS. CV+ does not lose predictive power due to a data-splitting procedure, but it is computationally more expensive.

Datasets. We select datasets to illustrate the performance of ACP in various scenarios: a simple classification problem with images (MNIST (LeCun 1998)), a more complex setting (CIFAR-10 (Krizhevsky, Nair, and Hinton 2009)), and a binary classification with tabular data (US Census (Ding et al. 2021)); details in Appendix C.2.

5.2 A warm-up example

We run an illustrative experiment for a CIFAR-10 test point picked uniformly at random. We consider a neural network with 3 layers of 100, 50, and 20 neurons; we refer to this network as MLP_C. Appendix C.3 gives implementation details.

Figure 5a shows the prediction set for a fixed $\varepsilon = 0.05$; we observe that, while all the methods output the true label, the prediction set of ACP (deleted) is the tightest (i.e., more efficient). We also report how the prediction set size changes w.r.t. ε , for ACP (Figure 5b) and for all methods (Figure 5c). As a way of comparing the curves, we include the AUC for the interval $\varepsilon \in [0, 0.2]$. ACP (deleted and ordinary) have the smallest AUC. Finally, for each method we report the highest ε for which the prediction set contains the true label. A higher value indicates that, for this test example, the method would still be accurate with an ε larger than 0.05, which would correspond to tighter prediction sets. Once again, ACP (deleted and ordinary) have the largest values. We show similar instances in Appendix E.2. In the next part, we observe this behavior generalizes to larger test sets.

We observe an unstable behavior in the predictions of RAPS and CV+: their prediction set size considerably oscillates as ε increases. The reason is that their prediction sets are not guaranteed to be nested; that is, $\varepsilon > \varepsilon'$ does not imply

that the prediction sets $\Gamma^\varepsilon \subseteq \Gamma^{\varepsilon'}$. Specifically, because RAPS and CV+ use randomness to decide whether to include a label in the set, the true label may appear and then disappear for a smaller significance level. This may not be desirable in some practical applications.¹ The prediction set for ACP and SCP monotonically decreases with ε , by construction.

5.3 Experimental setup

We evaluate the methods for five underlying models: three multilayer perceptrons with architectures (neurons per layer): 20-10 (MLP_A), 100 (MLP_B) and 100-50-20 (MLP_C); logistic regression (LR); and a convolutional neural network (CNN). In experiments with MNIST and CIFAR-10, the dimensionality is first reduced with an autoencoder (AE) in all settings except the CNN. We defer implementation details to Appendix C.3-C.4.

Considering these five settings enables comparing the methods both for underparametrized regimes (e.g., LR) and for better performing models (e.g., CNN). Note that CP’s guarantees hold regardless of whether the underlying model is misspecified. Further, observe that most of these models are non-convex, where the ERM optimization problem does not have a unique solution; this contradicts the IF assumption (Section 2). Nonetheless, our empirical results show that ACP works well – it performs better than the other proposals; in Section 7 we discuss relaxations of this assumption.

5.4 Results

For each experiment and method, we report averaged metrics over 100 test points; we also run statistical tests to check if differences are (statistically) significant.

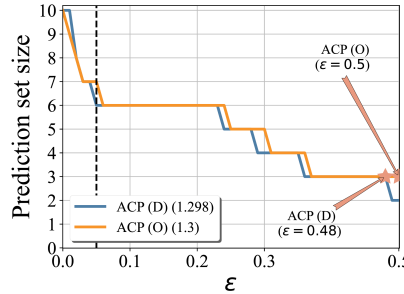
Prediction set size. We measure efficiency as the average prediction set size. We report this as a function of ε , discretized with a step $\Delta\varepsilon = 0.01$. Figures 6a and 6b show the average prediction set size in MNIST and CIFAR-10 for MLP_C. ACP (deleted and ordinary) consistently outperform all other methods; deleted is better than ordinary. ACP is significantly more efficient than RAPS and CV+. SCP and

¹RAPS allows a non-randomized version, although with a more conservative behavior and considerably larger prediction sets.

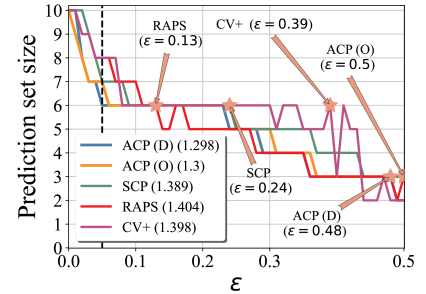


Method	Prediction set
ACP (D)	bird, cat, deer, dog, frog , horse
ACP (O)	plane, bird, cat, deer, dog, frog , horse
SCP	plane, bird, cat, deer, dog, frog , horse
RAPS	plane, bird, cat, deer, dog, frog , horse, truck
CV+	plane, auto, bird, cat, deer, dog, frog , horse

(a) Test image and prediction set ($\varepsilon = 0.05$)



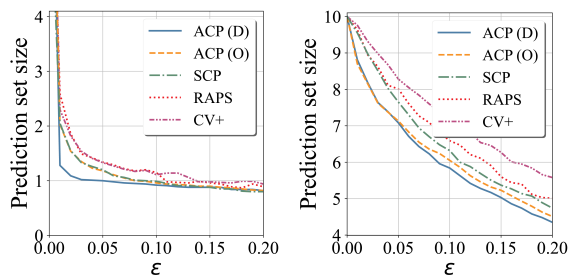
(b) Prediction set size (ACP)



(c) Prediction set size (all)

Figure 5: Prediction set for a fixed ε (5a), and prediction set size w.r.t. ε for ACP (5b) and comparing methods (5c). For each method, \star is the highest ε for which the prediction set includes the true label; higher is better. We also show the AUC in the interval $\varepsilon \in [0, 0.2]$; lower is better.

ACP (O) perform similarly on MNIST, but their difference is remarked on CIFAR-10; this suggests that SCP is a cheap effective alternative to ACP on relatively easier tasks. Appendix E.3 reports results for the rest of the models and for the US Census, showing similar behavior.



(a) MNIST

(b) CIFAR-10

Figure 6: Average prediction set size as a function of the significance level ε in MNIST (6a) and CIFAR-10 (6b) for MLP_C . Smaller prediction set size indicates better efficiency.

Efficiency AUC. We use an ε -independent metric to aid this comparison: the area under the curve (AUC) of the prediction set size in the interval $\varepsilon \in [0, 0.2]$; a smaller AUC means better efficiency. ACP (deleted or ordinary) prevails on all methods, datasets, and model combinations (Table 1). An exception is LR on US Census, where RAPS has a better efficiency than ACP and SCP; simpler tasks and models may be well served by the computationally efficient RAPS. Welch one-sided tests (reject with p-value < 0.1) confirm that both deleted and ordinary ACP are better than RAPS and CV+; they further show that either deleted or ordinary ACP are better than SCP on most tasks. We refer to Section 7 for directions to improve ACP’s performance.

Validity. As a way of interpreting why ACP performed better than the other methods, we measure their empirical error rate with a fixed $\varepsilon = 0.2$. Indeed, whilst all methods guarantee a probability of error of at most ε , a more conservative (i.e., smaller) empirical error may correspond to larger

US Census					
Model	ACP (D)	ACP (O)	SCP	RAPS	CV+
MLP_A	.301	.281	.302 \dagger	.318 $\star\dagger$.374 $\star\dagger$
MLP_B	.306	.304	.351 $\star\dagger$.351 $\star\dagger$.377 $\star\dagger$
MLP_C	.273	.275	.280	.299 $\star\dagger$.324 $\star\dagger$
LR	.276	.276	.284 $\star\dagger$.183	.344 $\star\dagger$
MNIST					
Model	ACP (D)	ACP (O)	SCP	RAPS	CV+
MLP_A	.252	.253	.261	.299 $\star\dagger$.322 $\star\dagger$
MLP_B	.220	.230	.233	.266 $\star\dagger$.277 $\star\dagger$
MLP_C	.198	.231	.230 \star	.258 $\star\dagger$.267 $\star\dagger$
LR	.385	.386	.379	.438 $\star\dagger$.467 $\star\dagger$
CNN	.175	.182	.237 $\star\dagger$.197 $\star\dagger$.199 $\star\dagger$
CIFAR-10					
Model	ACP (D)	ACP (O)	SCP	RAPS	CV+
MLP_A	1.261	1.259	1.281 $\star\dagger$	1.311 $\star\dagger$	1.373 $\star\dagger$
MLP_B	1.385	1.364	1.397 \dagger	1.416 $\star\dagger$	1.514 $\star\dagger$
MLP_C	1.226	1.250	1.327 $\star\dagger$	1.377 $\star\dagger$	1.475 $\star\dagger$
LR	1.409	1.411	1.419	1.436 $\star\dagger$	1.476 $\star\dagger$
CNN	.976	1.108	1.019	1.110 \star	1.467 $\star\dagger$

Table 1: Efficiency AUC ($\varepsilon \in [0, 0.2]$). The table indicates that differences in the AUC are statistically significant as compared to ACP (D) (\star) and ACP (O) (\dagger).

prediction sets. Table 2 shows the difference between the expected and the observed error rate on CIFAR-10 (i.e., $\varepsilon - \hat{\varepsilon}$). We observe that ACP achieves an error rate close to the significance level in most cases; this indicates this method fully exploits its error margin to optimize efficiency.² SCP shows a similar behavior. On the other hand, RAPS and CV+ are more conservative and tend to commit fewer errors. This means that RAPS and CV+ generate unnecessarily large prediction

²Note a randomized version of full CP, called smooth CP, ensures the error rate is exactly ε (instead of “at most ε ”). Herein, we use the standard, conservatively valid definition per Algorithm 1.

sets that, despite including the true label on average, result in lower efficiency. This behavior is consistent with analogous experiments on the US Census and MNIST datasets.

Model	ACP (D)	ACP (O)	SCP	RAPS	CV+
MLP _A	0.01	0.01	0	0.05	0.09
MLP _B	0.02	0.03	0.04	0.05	0.13
MLP _C	-0.01	0	0.02	-0.03	0.09
LR	0	0.03	-0.01	0.02	0.04
CNN	-0.01	0.01	-0.01	0.04	0.10

Table 2: Difference between the expected error ($\varepsilon = 0.2$) and the empirical error rate on CIFAR-10. A positive value indicates a conservative prediction set: the method could output tighter prediction sets without losing validity; a negative value is a validity violation, which may be due to statistical fluctuation (100 test points).

P-values fuzziness. Average prediction set size is a coarse criterion of efficiency: small variations in the algorithm may lead to substantially different prediction sets. An alternative efficiency criterion is fuzziness (Vovk et al. 2016), which measures how p-values distribute in the label space. Of the methods we considered, fuzziness can only be measured for ACP and SCP (RAPS and CV+ do not produce p-values). For every test point x , and computed p-values $\{p(x, \hat{y})\}_{\hat{y} \in \mathcal{Y}}$, fuzziness is the sum of the p-values minus the largest p-value: $\sum_{\hat{y} \in \mathcal{Y}} p(x, \hat{y}) - \max_{\hat{y} \in \mathcal{Y}} p(x, \hat{y})$; a small fuzziness is desirable. In Table 3, we observe that ACP (D) has a consistently better fuzziness than ACP (O) and SCP. We observe statistical significance of the results for 3 models in MNIST, and 2 models in CIFAR-10. Results for the US Census (Appendix D) are similar. As previously observed in Table 1, SCP performs better in logistic regression (MNIST); this makes it a good alternative for simpler underlying models.

6 Related work

Full CP (Vovk, Gammerman, and Shafer 2005) is notoriously expensive. Many alternatives have been proposed. Arguably the most prominent are SCP (Vovk, Gammerman, and Shafer 2005), CV+ (Romano, Sesia, and Candes 2020), RAPS (Angelopoulos et al. 2020), Cross-CP (Vovk 2012), aggregated CP (Carlsson, Eklund, and Norinder 2014), APS (Romano, Sesia, and Candes 2020), and the jackknife (Miller 1974;

Model	MNIST			CIFAR-10		
	ACP (D)	ACP (O)	SCP	ACP (D)	ACP (O)	SCP
MLP _A	.057	.059	.068*	1.796	1.832	1.849
MLP _B	.032	.041	.043*	1.967	2.050	2.132*
MLP _C	.012	.040	.044*	1.728	1.843	1.878*
LR	.187	.189	.183	2.269	2.280	2.332
CNN	.002	.002	.002	1.186	1.645	1.235

Table 3: Fuzziness of ACP and SCP on MNIST and CIFAR-10. A smaller fuzziness corresponds to more efficient prediction sets. The table indicates that differences in fuzziness are statistically significant as compared to ACP (D) (*) and ACP (O) (†).

Efron 1979). We compared ACP with the former three. Unlike full CP, all the above methods have weaker validity guarantees or they tend to attain less efficiency.

Cherubin, Chatzikokolakis, and Jaggi (2021) introduced exact optimizations for full CP for classification. Their method saves an order of magnitude in time complexity for many models, but is alas only applicable to models supporting incremental and decremental learning (e.g., k-NN). Crucially, it is unlikely extendable to neural networks

The closest in spirit to our approach is the Discriminative Jackknife (DJ) by Alaa and Van Der Schaar (2020), which uses IF to approximate jackknife+ confidence intervals for regression (Barber et al. 2021). We note several differences between ACP and DJ, besides their different goals (classification vs regression). While DJ approximates LOO w.r.t. the parameters, we introduce a *direct approach* to approximate the nonconformity scores in Equation 4. Whereas DJ only does decremental learning, which allows them to exploit Hessian-Vector-Products (Pearlmutter 1994), approximating full CP requires us to do both incremental *and* decremental learning (Algorithm 2). We also prove that our approximation error decreases w.r.t. the size of the training set.

7 Conclusion and Future Work

Full CP is a statistically sound method for providing performance guarantees on the outcomes of ML models. For classification tasks, CP generates prediction sets which contain the true label with a user-specified probability. Unfortunately, full CP is impractical to run for more than a few hundred training points. In this work, we develop ACP, a computationally efficient method which approximates full CP via influence functions; this strategy avoids the numerous recalculations that full CP requires. We prove that ACP is consistent: it approaches full CP as the training set grows. Our experiments support the use of ACP in practice.

There are many directions to improve ACP. For example, we assumed that the ERM solution is unique. While our approximation works well in practice, it would be a fruitful endeavour to relax this assumption; initial work towards this was done for IF by Koh and Liang (2017). Another direction is to build nonconformity scores on the *studentized* scheme, a middle way between deleted and ordinary (Vovk et al. 2017); this may further improve ACP’s prediction power. Future work can investigate when Condition 1 holds, and they can try to apply Theorem 2 to get direct error bounds on the coverage gap.

Finally, while we scale full CP to relatively large models, computing and inverting the Hessian becomes very expensive as the number of parameters increases. Recent tools to approximate the Hessian, like the Kronecker-factored Approximate Curvature (K-FAC) method (Martens and Grosse 2015; Ba, Grosse, and Martens 2017; Tanaka et al. 2020), might help further scale ACP to larger models like ResNets.

In conclusion, ACP helps scaling full CP to large datasets and ML models, for which running full CP would be impractical. Although split-based approaches like SCP and RAPS are less expensive to run, they do not attain the same efficiency as ACP. This makes the adoption of our method particularly appealing for critical real-world applications.

Acknowledgments

JA acknowledges support from the ETH AI Center. UB acknowledges support from DeepMind and the Leverhulme Trust via the Leverhulme Centre for the Future of Intelligence (CFI), and from the Mozilla Foundation. AW acknowledges support from a Turing AI Fellowship under grant EP/V025279/1, The Alan Turing Institute, and the Leverhulme Trust via CFI. GC acknowledges support from The Alan Turing Institute. The authors are grateful to Volodya Vovk, Pang Wei Koh and Manuel Gomez Rodriguez for useful comments and pointers.

References

- Alaa, A. M.; and Van Der Schaar, M. 2020. Discriminative Jackknife: Quantifying Uncertainty in Deep Learning via Higher-Order Influence Functions. In *Proceedings of the 37th International Conference on Machine Learning, ICML'20*. JMLR.org.
- Angelopoulos, A. N.; Bates, S.; Jordan, M.; and Malik, J. 2020. Uncertainty Sets for Image Classifiers using Conformal Prediction. In *International Conference on Learning Representations*.
- Ba, J.; Grosse, R. B.; and Martens, J. 2017. Distributed Second-Order Optimization using Kronecker-Factored Approximations. In *5th International Conference on Learning Representations, ICLR 2017, Toulon, France, April 24-26, 2017, Conference Track Proceedings*. OpenReview.net.
- Barber, R. F.; Candès, E. J.; Ramdas, A.; and Tibshirani, R. J. 2021. Predictive inference with the jackknife+. *The Annals of Statistics*, 49(1): 486 – 507.
- Basu, S.; Pope, P.; and Feizi, S. 2021. Influence Functions in Deep Learning Are Fragile. In *International Conference on Learning Representations*.
- Carlsson, L.; Eklund, M.; and Norinder, U. 2014. Aggregated Conformal Prediction. In *IFIP Advances in Information and Communication Technology*, volume 437, 231–240. ISBN 978-3-319-12567-1.
- Cherubin, G.; Chatzidakis, K.; and Jaggi, M. 2021. Exact Optimization of Conformal Predictors via Incremental and Decremental Learning. In Meila, M.; and Zhang, T., eds., *Proceedings of the 38th International Conference on Machine Learning*, volume 139 of *Proceedings of Machine Learning Research*, 1836–1845. PMLR.
- Ding, F.; Hardt, M.; Miller, J.; and Schmidt, L. 2021. Retiring Adult: New Datasets for Fair Machine Learning. In Beygelzimer, A.; Dauphin, Y.; Liang, P.; and Vaughan, J. W., eds., *Advances in Neural Information Processing Systems*.
- Efron, B. 1979. Bootstrap Methods: Another Look at the Jackknife. *Annals of Statistics*, 7: 1–26.
- Giordano, R.; Stephenson, W.; Liu, R.; Jordan, M.; and Broderick, T. 2019. A swiss army infinitesimal jackknife. In *The 22nd International Conference on Artificial Intelligence and Statistics*, 1139–1147. PMLR.
- Hampel, F. R. 1974. The influence curve and its role in robust estimation. *Journal of the american statistical association*, 69(346): 383–393.
- Koh, P. W.; and Liang, P. 2017. Understanding black-box predictions via influence functions. In *International Conference on Machine Learning*, 1885–1894. PMLR.
- Koh, P. W. W.; Ang, K.-S.; Teo, H.; and Liang, P. S. 2019. On the accuracy of influence functions for measuring group effects. In *Advances in Neural Information Processing Systems*, 5254–5264.
- Krizhevsky, A.; Nair, V.; and Hinton, G. 2009. CIFAR-10.
- LeCun, Y. 1998. The MNIST database of handwritten digits. <http://yann.lecun.com/exdb/mnist/>.
- Lei, J. 2019. Fast exact conformalization of the lasso using piecewise linear homotopy. *Biometrika*, 106(4): 749–764.
- Lin, Z.; Trivedi, S.; and Sun, J. 2021. Locally Valid and Discriminative Prediction Intervals for Deep Learning Models. In Ranzato, M.; Beygelzimer, A.; Dauphin, Y.; Liang, P.; and Vaughan, J. W., eds., *Advances in Neural Information Processing Systems*, volume 34, 8378–8391. Curran Associates, Inc.
- Linusson, H.; Johansson, U.; Boström, H.; and Löfström, T. 2014. Efficiency Comparison of Unstable Transductive and Inductive Conformal Classifiers. In *AIAI Workshops*.
- Martens, J.; and Grosse, R. 2015. Optimizing Neural Networks with Kronecker-Factored Approximate Curvature. In *Proceedings of the 32nd International Conference on International Conference on Machine Learning - Volume 37, ICML'15*, 2408–2417. JMLR.org.
- Miller, R. G. 1974. The jackknife—a review. *Biometrika*, 61: 1–15.
- Ndiaye, E. 2022. Stable Conformal Prediction Sets. In *International Conference on Machine Learning*, 16462–16479. PMLR.
- Ndiaye, E.; and Takeuchi, I. 2019. Computing full conformal prediction set with approximate homotopy. *Advances in Neural Information Processing Systems*, 32.
- Noureddinov, I.; Melluish, T.; and Vovk, V. 2001. Ridge regression confidence machine. In *ICML*, 385–392. Citeseer.
- Papadopoulos, H.; Proedrou, K.; Vovk, V.; and Gammerman, A. 2002. Inductive Confidence Machines for Regression. In Elomaa, T.; Mannila, H.; and Toivonen, H., eds., *Machine Learning: ECML 2002*. Berlin, Heidelberg: Springer Berlin Heidelberg.
- Papadopoulos, H.; Vovk, V.; and Gammerman, A. 2011. Regression conformal prediction with nearest neighbours. *Journal of Artificial Intelligence Research*, 40: 815–840.
- Pearlmutter, B. A. 1994. Fast exact multiplication by the Hessian. *Neural computation*, 6(1): 147–160.
- Pedregosa, F.; Varoquaux, G.; Gramfort, A.; Michel, V.; Thirion, B.; Grisel, O.; Blondel, M.; Prettenhofer, P.; Weiss, R.; Dubourg, V.; Vanderplas, J.; Passos, A.; Cournapeau, D.; Brucher, M.; Perrot, M.; and Duchesnay, E. 2011. Scikit-learn: Machine Learning in Python. *Journal of Machine Learning Research*, 12: 2825–2830.
- Romano, Y.; Sesia, M.; and Candès, E. 2020. Classification with Valid and Adaptive Coverage. *Advances in Neural Information Processing Systems*, 33: 3581–3591.

Shafer, G.; and Vovk, V. 2008. A tutorial on conformal prediction. *Journal of Machine Learning Research*, 9(Mar): 371–421.

Tanaka, H.; Kunin, D.; Yamins, D. L.; and Ganguli, S. 2020. Pruning neural networks without any data by iteratively conserving synaptic flow. In Larochelle, H.; Ranzato, M.; Hadsell, R.; Balcan, M.; and Lin, H., eds., *Advances in Neural Information Processing Systems*, volume 33, 6377–6389. Curran Associates, Inc.

Vovk, V. 2012. Cross-conformal predictors. *Annals of Mathematics and Artificial Intelligence*, 74.

Vovk, V.; Fedorova, V.; Nouretdinov, I.; and Gammerman, A. 2016. Criteria of efficiency for conformal prediction. In *Symposium on conformal and probabilistic prediction with applications*, 23–39. Springer.

Vovk, V.; Gammerman, A.; and Shafer, G. 2005. *Algorithmic learning in a random world*. Springer Science & Business Media.

Vovk, V.; Shen, J.; Manokhin, V.; and Xie, M.-g. 2017. Non-parametric predictive distributions based on conformal prediction. In *Conformal and Probabilistic Prediction and Applications*, 82–102. PMLR.

A Additional information about ACP

A.1 Ordinary Full CP and ACP

Algorithm 3: Full CP - Ordinary

```

1: for  $x$  in test points do
2:   for  $\hat{y} \in \mathcal{Y}$  do
3:      $\hat{z} = (x, \hat{y})$ 
4:      $\theta_{Z \cup \{\hat{z}\}} = \operatorname{argmin}_{\hat{\theta} \in \Theta} R(Z \cup \{\hat{z}\}, \hat{\theta})$ 
5:     for  $z_i \in Z \cup \{\hat{z}\}$  do
6:        $\alpha_i = \ell(z_i, \theta_{Z \cup \{\hat{z}\}})$ 
7:     end for
8:      $p_{(x, \hat{y})} = \frac{\#\{i=1, \dots, N+1 : \alpha_i \geq \alpha_{N+1}\}}{N+1}$ 
9:     If  $p_{(x, \hat{y})} > \varepsilon$ , include  $\hat{y}$  in prediction set  $\Gamma_x^\varepsilon$ 
10:  end for
11: end for

```

Algorithm 3 shows the Full CP algorithm constructed for a nonconformity measure defined on an ordinary scheme. ACP with the ordinary prediction can be defined similarly to the deleted one as follows. Once again, we can use the direct or indirect approach.

Indirect approach. Let $\tilde{\theta}_{Z \cup \{\hat{z}\}} \equiv \theta_Z + I_{\theta_Z}(\hat{z})$. Then:

$$\alpha_i \approx \ell(z_i, \tilde{\theta}_{Z \cup \{\hat{z}\}}). \quad (5)$$

Direct approach.

$$\begin{aligned} \alpha_i &\approx \tilde{\ell}(z_i, \theta_{Z \cup \{\hat{z}\}}) \\ &\equiv \ell(z_i, \theta_Z) + I_\ell(z_i, \hat{z}) \end{aligned} \quad (6)$$

Observe that the only difference w.r.t. ACP (deleted) is that here we only need to add the influence of \hat{z} ; that is, we do not need to remove the influence of $z_i \in Z \cup \{\hat{z}\}$. This spares the very costly LOO procedure of retraining the model, which makes this method significantly more computationally efficient.

A.2 Time complexity: Full CP Vs ACP

Predicting m test points via full CP in an l -label classification setting costs $\mathcal{O}(nlm(T_n + P))$, where T_n is the cost of training a model on n training points, and P is the cost of making a prediction with it.

The ACP procedure is split into two steps: training and prediction. Training costs $\mathcal{O}(T_n + H_n + n(G_n + P))$, where H_n and G_n are the costs of computing the Hessian inverse and a gradient, respectively. We denote the dependency on the training set size with the subscript n . Computing a prediction for m points costs $\mathcal{O}(lm(G_n + nI_n + P))$, where I_n is the (usually small) cost of computing the influence; this gives an order speed-up over CP.

	Train	Predict
Full CP	N/A	$nlm(T_n + P)$
ACP	$T_n + H_n + n(G_n + P)$	$lm(G_n + nI_n + P)$

Table 4: Time complexities for full CP and ACP.

As an illustrative example, let us assume a standard classification problem with l labels, a training set with size N , and a smaller test set M , where we fit a 3-layers neural network. The full CP algorithm would retrain the model $l \times N$ times per **each** test point in M . This is infeasible for relatively large datasets with, e.g., more than 1000 points, either in the training or the test set. Conversely, ACP only needs to train the model once, compute the Hessian inverse and the N gradients (training step). Although inverting the Hessian requires $\mathcal{O}(W^3)$ operations, this is expected to be significantly faster than full CP’s retraining procedure for this standard scenario. ACP only needs access to the gradient of the test point to inexpensively compute the IF (prediction step).

We measured the running times in the synthetic dataset (Appendix C) with 50 features, 1000 training points, and 100 test points. As indicative figures, running full CP in this setting took approximately 5 days, whereas ACP took less than 1 hour (CPU times with an Intel Core i7-8750H).

A.3 Space complexity

ACP requires storing the Hessian inverse, i.e., $\mathcal{O}(W^2)$ with W being the number of parameters, and one gradient per training point, i.e., $\mathcal{O}(nW)$. Full CP stores the full training set.

A.4 Additional discussion on the nonconformity score

Any nonconformity measure $A : (\mathcal{X} \times \mathcal{Y}) \times (\mathcal{X} \times \mathcal{Y})^N \rightarrow \mathbf{R}$ defines a conformal predictor (CP); given an example $x \in \mathcal{X}$ and a significance level ε , this predictor generates a set that contains the true label $y \in \mathcal{Y}$ with probability $1 - \varepsilon$. The intuition here is that y will have a value that makes the pair (x, y) conform with the previous examples; the validity is therefore conditioned on the *training set*. The nonconformity score is simply a measure of how different a new example is from old examples. In a general setting, the nonconformity measure is arbitrary; the validity guarantees always hold, e.g., a random score will still generate valid prediction sets, although likely with low efficiency. Whether a function A is an appropriate nonconformity score will always be open to discussion since it greatly depends on the context (Vovk, Gammerman, and Shafer 2005).

ACP (Algorithm 2) restricts the nonconformity score to be the loss at a point. Although the instance-wise loss might be suboptimal, the underlying algorithm is arbitrary. Shafer and Vovk (2008) point out that the score choice is relatively unimportant and that the critical step in the CP framework is determining the underlying classifier. It is therefore not expected that ACP degrades its efficiency by using the loss as score as long as the wrapped classifier is appropriate.

B Proofs

B.1 ACP consistency

We first declare the following set of assumptions introduced and thoroughly discussed by Giordano et al. (2019).

Assumption 1.

- For all $\theta \in \Theta$ and all $z_i \in Z$, $\nabla_{\theta} \ell(z_i, \theta)$ is continuously differentiable in θ .
- For all $\theta \in \Theta$, the Hessian H_{θ} is non-singular with $\sup_{\theta \in \Theta} \|H_{\theta}^{-1}\|_{op} < \infty$.
- \exists finite constants C_g, C_h s.t. $\sup_{\theta \in \Theta} \frac{1}{\sqrt{N}} \|\nabla_{\theta} \ell(z, \theta)\|_2 \leq C_g$ and $\sup_{\theta \in \Theta} \frac{1}{\sqrt{N}} \|\nabla_{\theta}^2 \ell(z, \theta)\|_2 \leq C_h$.
- Let $h(\theta) = \nabla_{\theta}^2 \ell(z, \theta)$. There exists $\Delta_{\theta} > 0$ and a finite constant L_h such that $\|\theta - \theta_Z\|_2 \leq \Delta_{\theta}$ implies that $\frac{\|h(\theta) - h(\theta_Z)\|_2}{\sqrt{N}} \leq L_h \|\theta - \theta_Z\|_2$.

To prove Theorem 2 we exploit the following result by Giordano et al. (2019): Let $\tilde{\theta}_{Z \setminus \{z_i\}} = \theta_Z - I_{\theta}(z_i, z_i)$ be the approximation of $\theta_{Z \setminus \{z_i\}}$ obtained from Equation 1.

Theorem 4 (Consistency of $\tilde{\theta}_{Z \setminus \{z_i\}}$ (Giordano et al. 2019)). *Under Assumption 1, for every N there is a constant C s.t., for every $z_i \in Z$:*

$$\begin{aligned} \|\tilde{\theta}_{Z \setminus \{z_i\}} - \theta_{Z \setminus \{z_i\}}\|_2 &\leq C \frac{\|g\|_{\infty}^2}{N^2} \\ &\leq C \frac{\max\{C_g, C_h\}^2}{N} \end{aligned}$$

(Note, the result by Giordano et al. is stated more generally for the case of leave k out; we only report its LOO version. Also, the general case requires 2 further assumptions, which we omit as they are always satisfied for LOO.)

We now restate and prove the consistency of ACP.

Theorem 2 (Consistency of approximate full CP). *Under Assumption 1 and Condition 1, let $\alpha_i = \ell(z_i, \theta_{Z \cup \{\hat{z}\} \setminus \{z_i\}})$, and suppose ℓ is K -Lipschitz. For every N there is a constant C such that for every $z_i \in Z \cup \{\hat{z}\}$:*

$$|\tilde{\ell}(z_i, \theta_{Z \cup \{\hat{z}\} \setminus \{z_i\}}) - \alpha_i| \leq KC \frac{\max\{C_g, C_h\}^2}{N},$$

for finite constants C_g, C_h s.t. $\sup_{\theta \in \Theta} \frac{1}{\sqrt{N}} \|\nabla_{\theta} \ell(z, \theta)\|_2 \leq C_g$ and $\sup_{\theta \in \Theta} \frac{1}{\sqrt{N}} \|\nabla_{\theta}^2 \ell(z, \theta)\|_2 \leq C_h$.

Proof. First, from Theorem 4 (Giordano et al. 2019) we have that, for every N there exists constants C and C' such that:

$$\begin{aligned} \|\theta_{Z \cup \{\hat{z}\}} - I_{\theta}(z_i) - \theta_{Z \cup \{\hat{z}\} \setminus \{z_i\}}\|_2 &\leq C \frac{\max\{C_g, C_h\}^2}{N} \\ \|\theta_{Z \cup \{\hat{z}\}} - I_{\theta}(\hat{z}) - \theta_Z\|_2 &\leq C' \frac{\max\{C_g, C_h\}^2}{N}; \end{aligned}$$

observe that the second expression is obtained by removing \hat{z} from the training data of a model trained on $Z \cup \{\hat{z}\}$.

Fix $z_i \in Z \cup \{\hat{z}\}$.

$$\begin{aligned}
|\tilde{\ell}(z_i, \theta_{Z \cup \{\hat{z}\} \setminus \{z_i\}}) - \ell(z_i, \theta_{Z \cup \{\hat{z}\} \setminus \{z_i\}})| &\leq |\ell(z_i, \tilde{\theta}_{Z \cup \{\hat{z}\} \setminus \{z_i\}}) - \ell(z_i, \theta_{Z \cup \{\hat{z}\} \setminus \{z_i\}})| \\
&= |\ell(z_i, \tilde{\theta}_{Z \cup \{\hat{z}\} \setminus \{z_i\}}) - \ell(z_i, \theta_{Z \cup \{\hat{z}\} \setminus \{z_i\}})| \\
&\leq K \|\tilde{\theta}_{Z \cup \{\hat{z}\} \setminus \{z_i\}} - \theta_{Z \cup \{\hat{z}\} \setminus \{z_i\}}\|_2 \\
&= K \|\theta_Z + I_\theta(\hat{z}) - I_\theta(z_i) - \theta_{Z \cup \{\hat{z}\} \setminus \{z_i\}}\|_2 \\
&\leq K \|\theta_{Z \cup \{\hat{z}\}} - I_\theta(z_i) - \theta_{Z \cup \{\hat{z}\} \setminus \{z_i\}}\|_2 + \|\theta_{Z \cup \{\hat{z}\}} - I_\theta(\hat{z}) - \theta_Z\|_2 \\
&\leq K(C + C') \frac{\max\{C_g, C_h\}^2}{N}
\end{aligned}$$

First step applies Condition 1, third step uses Lipschitz continuity, fourth step uses triangle inequality, and the final step uses Theorem 4. \square

B.2 Dependence on the regularization parameter λ

Our result on the effect of the regularization parameter on the approximation error of ACP (Theorem 3) is an extension of a result by Koh et al. (2019) on the approximation error of IF for LOO.

Background on result by Koh et al. (2019) The LOO loss can be written as

$$\ell(z_i, \theta_{Z \setminus \{z_i\}}) = \ell(z_i, \theta_Z) - I_\ell^*(z_i, z_i) \approx \ell(z_i, \theta_Z) - I_\ell(z_i, z_i),$$

where $I_\ell^*(z_i, z_i)$ is defined to be the true influence of training point $z_i \in Z$ on the loss of the model at z_i . For simplicity, we omit the arguments of I_ℓ when clear from the context. In the following, we assume θ is the minimizer of an ERM problem with regularization parameter λ .

Koh et al. (2019) decompose the influence function error into Newton-actual error (E_A) and Newton-influence error (E_I):

$$I_\ell^* - I_\ell = E_A + E_I$$

with $E_A \equiv I_\ell^* - I_\ell^N$, and $E_I \equiv I_\ell^N - I_\ell$. Here I_ℓ^N is the Newton approximation of the true influence I_ℓ^* .

Koh et al. (2019) show that E_A decreases with $\mathcal{O}(\frac{1}{\lambda^3})$, and they observed that its value tends to be negligible in practice.

Proposition 5 (Koh et al. (2019)). *Assume that ℓ is C_f -Lipschitz and that the Hessian is C_H -Lipschitz. Further, assume the third derivative of ℓ exists and that it is bounded in norm by $C_{f,3}$. The influence on the self-loss is such that:*

$$I_\ell(z_i) + E_{f,3} \leq I_\ell^N(z_i) \leq \left(1 + \frac{3\sigma_{max}}{2\lambda} + \frac{\sigma_{max}^2}{2\lambda^2}\right) I_\ell(z_i) + E_{f,3}(z_i).$$

Furthermore:

$$|E_{f,3}(z_i)| \leq \frac{C_{f,3}C_\ell^3}{6(\sigma_{min} + \lambda)^3}.$$

Extension to ACP If we assume E_A to be negligible, we obtain that $I_\ell^* \approx I_\ell^N$. Further, ignoring $\mathcal{O}(\lambda^{-3})$ terms, Proposition 5 gives:

$$I_\ell \leq I_\ell^* \leq g(\lambda)I_\ell,$$

that is (by subtracting each term from $\ell(z_i, \theta_Z)$):

$$\ell(z_i, \theta_Z) - g(\lambda)I_\ell(z_i, z_i) \leq \ell(z_i, \theta_{Z \setminus \{z_i\}}) \leq \ell(z_i, \theta_Z) - I_\ell(z_i, z_i) = \tilde{\ell}(z_i, \theta_{Z \setminus \{z_i\}}).$$

Note, however, that this result only applies to the LOO loss. We use the following simplifying assumption to extend the above result to ACP.

Assumption 2. For all z_i and \hat{z} :

$$I_\ell^*(z_i, \hat{z}) \approx I_\ell(z_i, \hat{z})$$

We can now restate and prove our result.

Theorem 3 (Approximation goodness w.r.t. regularizer). *Suppose the model is trained via ERM with regularization parameter λ . Under the assumptions of Proposition 5, Assumption 2, and neglecting $\mathcal{O}(\lambda^{-3})$ terms, we have the following cone constraint between the true nonconformity measure $\alpha_i = \ell(z_i, \theta_{Z \cup \{\hat{z}\} \setminus \{z_i\}})$ and its direct approximation $\tilde{\ell}(z_i, \theta_{Z \cup \{\hat{z}\} \setminus \{z_i\}}) \equiv \ell(z_i, \theta_Z) + I_\ell(z_i, \hat{z}) - I_\ell(z_i, z_i)$, where $g(\lambda) = (1 + 3\sigma_{max}/2\lambda + \sigma_{max}^2/2\lambda^2)$, and σ_{max} is the maximum eigenvalue of the Hessian H :*

$$\ell(z_i, \theta_Z) + I_\ell(z_i, \hat{z}) - g(\lambda)I_\ell(z_i, z_i) \leq \alpha_i \leq \tilde{\ell}(z_i, \theta_{Z \cup \{\hat{z}\} \setminus \{z_i\}}).$$

Proof. Koh et al. show that (ignoring $O(\lambda^{-3})$ terms):

$$I_\ell(z_i) \leq I_\ell^{\mathcal{N}}(z_i) \leq \left(1 + \frac{3\sigma_{max}}{2\lambda} + \frac{\sigma_{max}^2}{2\lambda^2}\right) I_\ell(z_i).$$

(For a definition of all the terms please refer to Appendix B.2.) Ignoring $O(\lambda^{-3})$ terms, we apply this to the loss:

$$\ell(z_i, \theta_Z) - g(\lambda)I_\ell(z_i, z_i) \leq \ell(z_i, \theta_{Z \setminus \{z_i\}}) \leq \ell(z_i, \theta_Z) - I_\ell(z_i, z_i)$$

We apply this to the augmented training set $Z \cup \{\hat{z}\}$ (now z_i ranges in $Z \cup \{\hat{z}\}$):

$$\ell(z_i, \theta_{Z \cup \{\hat{z}\}}) - g(\lambda)I_\ell(z_i, z_i) \leq \ell(z_i, \theta_{Z \cup \{\hat{z}\} \setminus \{z_i\}}) \leq \ell(z_i, \theta_{Z \cup \{\hat{z}\}}) - I_\ell(z_i, z_i).$$

By using Assumption 2, replace $\ell(z_i, \theta_{Z \cup \{\hat{z}\}})$ with $\ell(z_i, \theta_Z) + I_\ell(z_i, \hat{z})$. This concludes the proof. \square

C Experimental details

C.1 Synthetic data (Section 4)

We generate synthetic data for a binary classification problem using `scikit-learn`'s `make_classification()` (Pedregosa et al. 2011). We sample points from four Gaussian-distributed clusters (two per class).

C.2 Real data (Section 5)

Follows a brief description of the datasets we used and of their pre-processing.

- **MNIST**: we use 60,000 images for training and 10,000 for testing from the MNIST dataset (LeCun 1998) – from which we take the first 100 test points. The 28×28 grayscale images represent handwritten digits between 0 and 9. In all settings except the CNN, these images are standardized in the interval $[0, 1]$ by dividing the pixel intensities by 255.
- **CIFAR-10**: we use 50,000 images for training and 10,000 for testing from the CIFAR-10 dataset (Krizhevsky, Nair, and Hinton 2009) – from which we take the first 100 test points. These correspond to images from 10 mutually exclusively classes. We also standardize them in the interval $[0, 1]$ (except in setting CNN).
- **US Census**: we use the ACSIncome data for the state of New York from the US Census dataset (Ding et al. 2021). Each data point represents an individual above the age of 16, who reported usual working hours of at least 1 hour per week in the past year, and an income of at least \$100. Ten features characterize each point, and the task consists of predicting whether the individual's income is above \$50,000. We split the dataset of 103,021 points and keep the 90% (92,718) for training. We take 100 test points from the remaining.

C.3 Implementation details

We use dense layers with Rectified Linear Units (ReLU) as nonlinear activation functions in all the models. Settings MLP_A , MLP_B and MLP_C are based on multilayer perceptrons with different widths and depths, LR uses logistic regression, and CNN a convolutional neural network. All models are trained with Adam for a maximum of 200 epochs. We fix a learning rate of 0.001, minibatches of size 100, and an early stopping based on a 20% validation split. We also set a regularization $\lambda = 10^{-5}$. We use a cross-entropy loss function.

We use an autoencoder (AE) to reduce the dimensionality of MNIST and CIFAR-10 for settings MLP_A , MLP_B , MLP_C , and LR. The AE uses a symmetric encoder-decode architecture with two dense layers of 128 and 64 neurons, separated by dropout with $p = 0.2$ and ReLU activations.

We now give specific details of each setting:

- **MLP_A** : two layers, the first with 20 and the second with 10 neurons. The embedding size for the AE is 8.
- **MLP_B** : one layer with 100 neurons. Embedding size of 16.
- **MLP_C** : three layers with 100, 50, and 20 neurons. Embedding size of 32.
- **LR**: embedding size of 8.
- **CNN**: two convolutional layers with 16 and 32 kernels of size 5, respectively. They include a ReLU activation and max-pool layer with kernel size 4. A multilayer-perceptron makes the classification.

C.4 Design choices for the methods

Here we comment on some design choices that we made when including the competing methods.

- **SCP**: we fix a calibration split of 20%, as advised in (Linusson et al. 2014). We obtain the nonconformity scores by fitting the model in the proper training set and computing the loss for the calibration data.

- **RAPS**: we fix a calibration split of 20%. We use the randomized version of the algorithm, and we do not allow zero sets (i.e., we use the default version in (Angelopoulos et al. 2020)). The randomized version, although slightly unstable, provides a less conservative coverage. The parameters “kreg” and “lamda” are picked in an optimal fashion that minimizes the prediction set size. We therefore compare ACP to the most efficient version of RAPS.
- **CV+**: we set $K = 5$ as the number of folds for the cross-validation.

For ACP, we add a damping term of $\lambda = 0.01$ to the Hessian to enforce positive eigenvalues. This is equivalent to an l2-regularisation.

D Fuzziness comparison

Table 5 shows the fuzziness of ACP and SCP on the US Census dataset. Results match the behavior observed for MNIST and CIFAR-10 (Section 5).

		US Census		
Model		ACP (D)	ACP (O)	SCP
MLP _A		.1086	.0844	.1121 [†]
MLP _B		.1144	.1366	.2173*
MLP _C		.0733	.0768	.0741
LR		.0781	.0782	.0885

Table 5: Fuzziness of ACP and SCP on US Census. A smaller fuzziness corresponds to more efficient prediction sets.

*Differences in the fuzziness are statistically significant compared to ACP (D). [†]Differences are significant compared to ACP (O).

E Further results

E.1 Additional experiments with synthetic data

We run additional experiments on synthetic data to further support the theory in Section 3.2. Specifically, we show how ACP’s p-values approximate Full CP’s as the training set increases, for different numbers of features and regularization strengths. We also compute the Kendall tau distance between the p-values rankings.

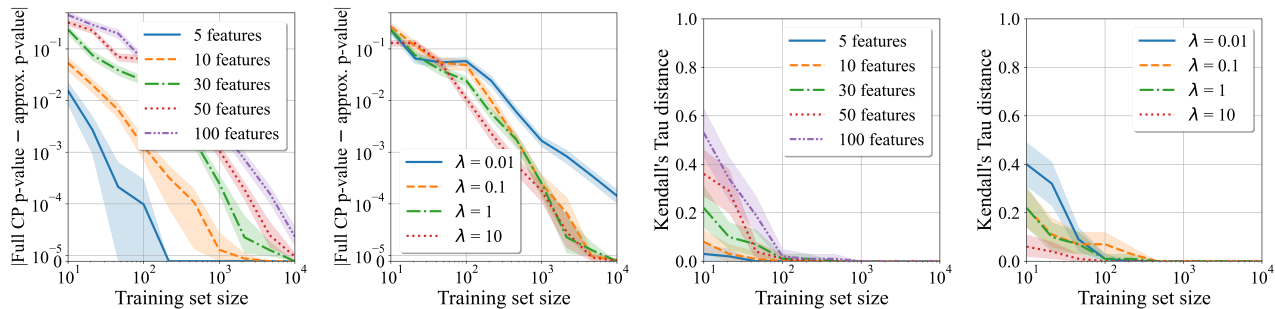


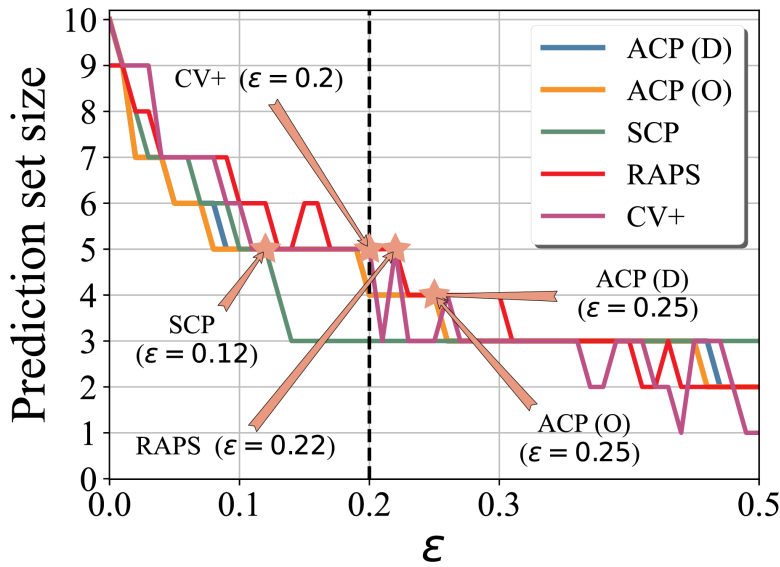
Figure 7: Additional experiments on synthetic data. We further support that ACP generates the same p-values as full CP as the training set increases.

E.2 Additional motivating examples

We include additional motivating examples with specific instances from CIFAR-10 and MNIST for setting MLP_C.

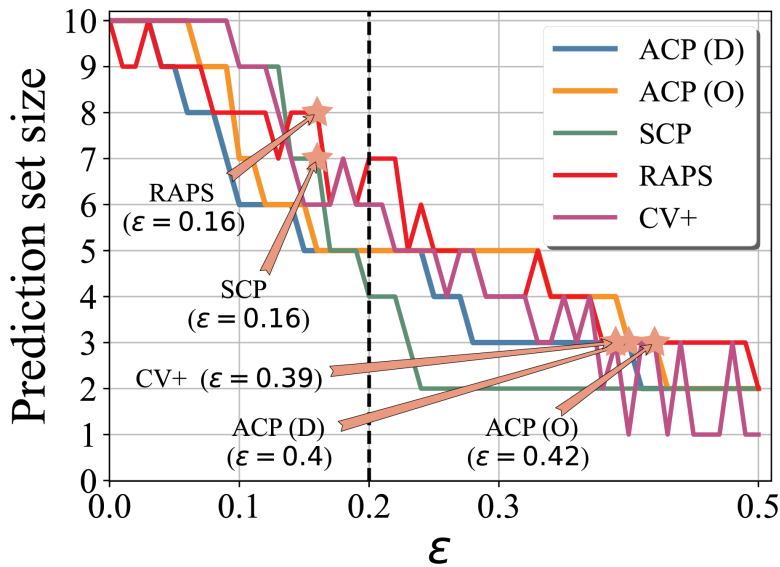
E.3 Additional curves

Figure 13 plots the average prediction set size w.r.t the significance ε for all combinations of settings (MLP_A, MLP_B, MLP_C, LR, CNN) and datasets (MNIST, CIFAR-10, US Census).



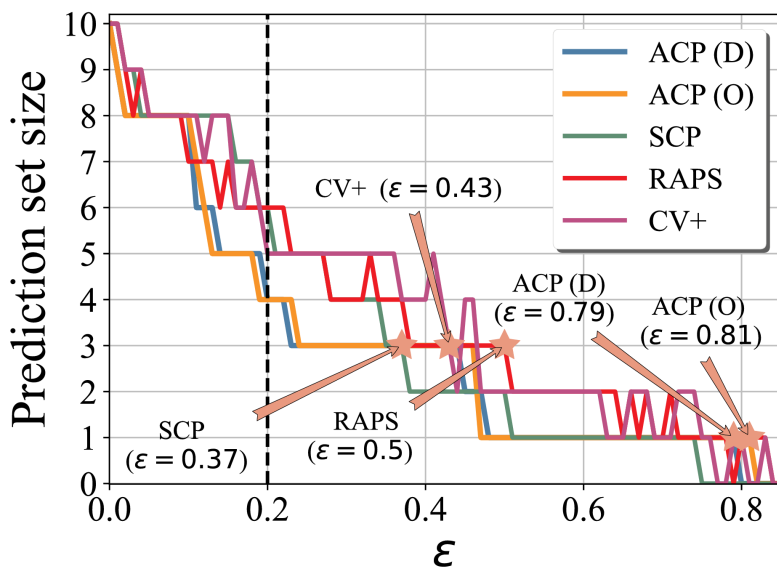
$\varepsilon = 0.2$	
Method	Prediction set
ACP (D)	bird, cat , deer, frog
ACP (O)	bird, cat , deer, frog
SCP	bird, deer, frog
RAPS	bird, cat , deer, dog, frog
CV+	bird, cat , deer, dog, frog

Figure 8: Prediction set size as a function of ε for a specific instance from CIFAR-10. We indicate with a star the point (ε) at which each method starts containing the true label. ACP (D) and ACP (O) are the *fastest*, meaning that they include the true label earlier than the rest of methods (i.e., at higher ε). For a typical significance $\varepsilon = 0.2$, the prediction sets generated by both methods are the smallest that contain the true label. RAPS and CV+ are more conservative, while SCP fails to include it.



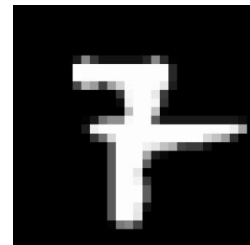
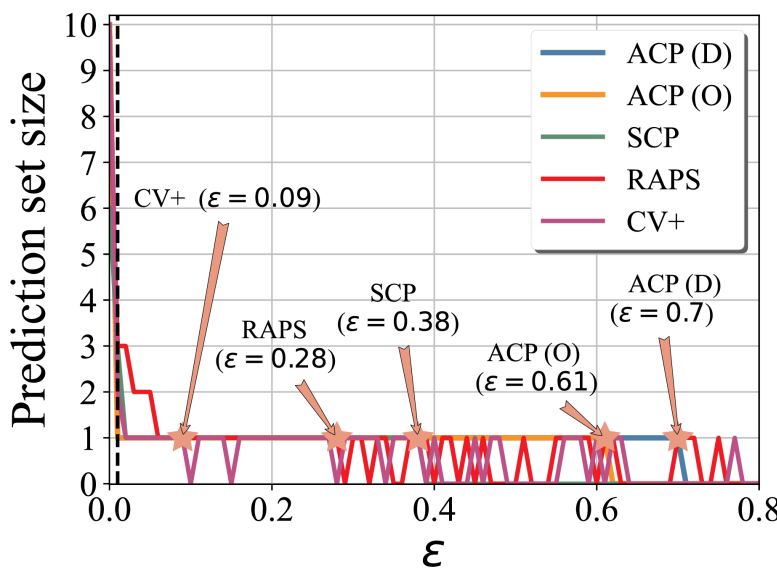
$\varepsilon = 0.2$	
Method	Prediction set
ACP (D)	auto, cat, frog, horse , truck
ACP (O)	auto, cat, frog, horse , truck
SCP	auto, deer, frog, truck
RAPS	plane, auto, bird, deer, frog, ship, truck
CV+	plane, auto, deer, frog, horse , truck

Figure 9: Additional motivating example in CIFAR-10. For a typical significance $\varepsilon = 0.2$, ACP (D) and ACP (O) yield the smallest prediction sets that contain the true label. ACP (D) and ACP (O) are the first to consider the true label.



$\epsilon = 0.2$	
Method	Prediction set
ACP (D)	cat, deer, frog , horse
ACP (O)	cat, deer, frog , horse
SCP	cat, deer, dog, frog , horse, truck
RAPS	cat, deer, dog, frog , horse, truck
CV+	cat, deer, dog, frog , horse

Figure 10: Additional motivating example in CIFAR-10. For a typical significance $\epsilon = 0.2$, all methods include the true label, ACP (D) and ACP (O) yielding the smallest prediction sets. ACP (D) and ACP (O) are the first to consider the true label.



$\epsilon = 0.01$	
Method	Prediction set
ACP (D)	<u>7</u>
ACP (O)	<u>7</u>
SCP	4, <u>7</u> , 8
RAPS	4, <u>7</u> , 8
CV+	1, <u>7</u>

Figure 11: Additional motivating example in MNIST. For a typical significance $\epsilon = 0.01$, all methods include the true label, ACP (D) and ACP (O) yielding the smallest prediction sets. ACP (D) and ACP (O) are also the first to consider the true label.

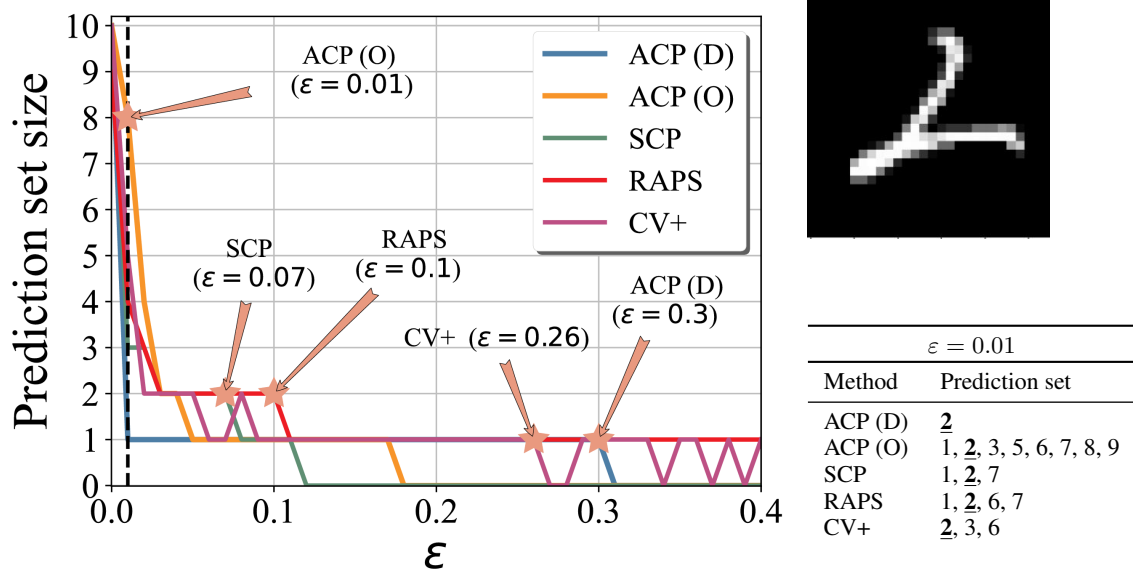


Figure 12: Additional motivating example in MNIST. For a typical significance $\epsilon = 0.01$, all methods include the true label, ACP (D) yielding the smallest prediction sets. ACP (D) is the first method to consider the true label, followed by CV+. ACP (O) builds the largest set and is the *slowest* to consider the true label.

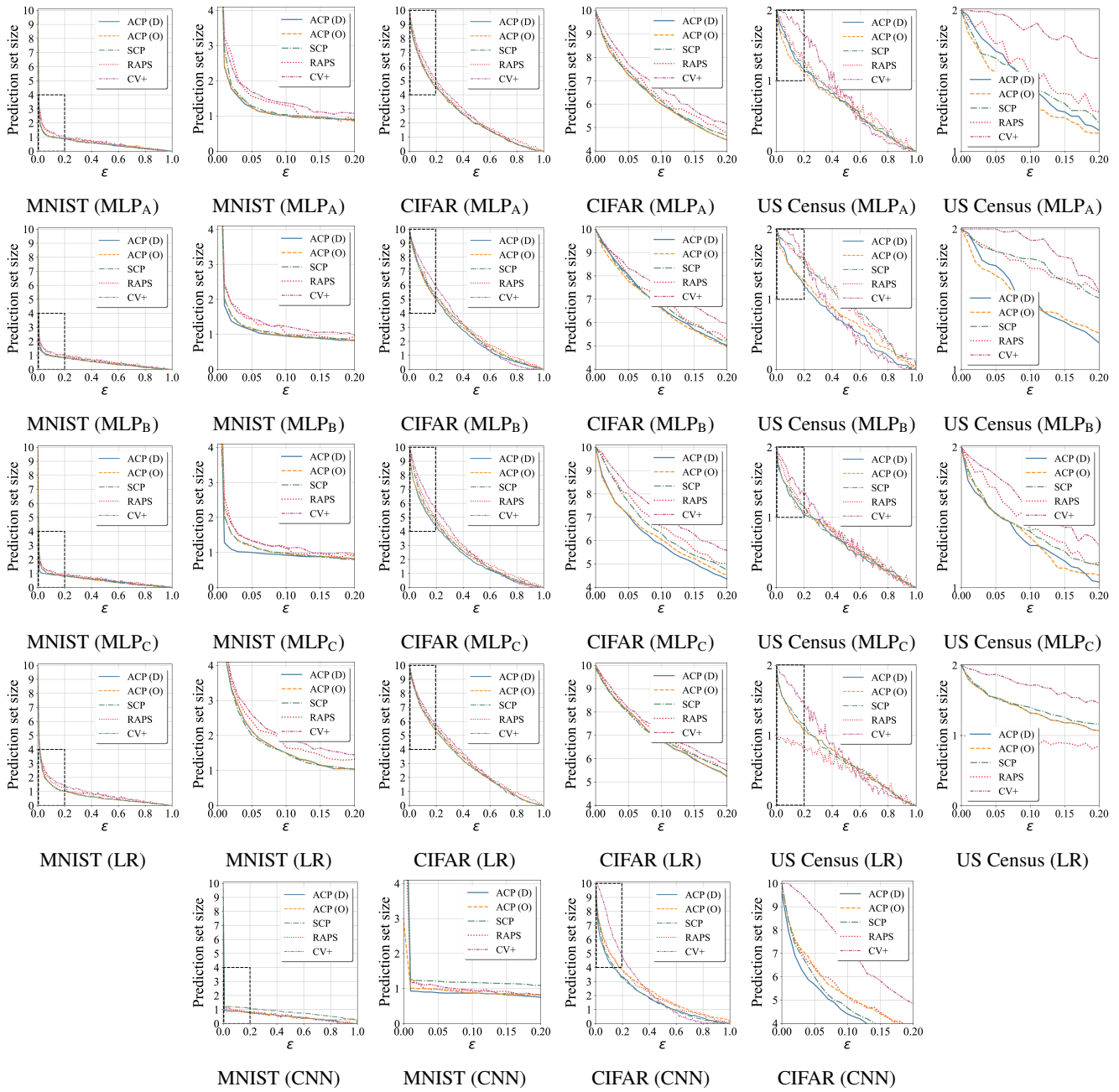


Figure 13: Average prediction set size w.r.t the significance level ϵ for all settings and datasets. We show both the full curve and the corresponding to the interval of interest $\epsilon \in [0, 0.2]$